

SPATIAL RESOLUTION OF SYSTEMS OF VISION THROUGH THE ATMOSPHERE

V.V. Belov and I.Yu. Makushkina

*Institute of Atmospheric Optics,
Siberian Branch of the Russian Academy of Sciences, Tomsk*

Received May 26, 1992

A criterion for spatial resolution is examined for viewing through the atmosphere with illumination from an external source. The dependence of the spatial resolution of a vision system on its optical and geometric parameters is analyzed for two objects of sufficiently arbitrary shape. Certain recommendations for the choice of optimum viewing conditions against the above-considered criterion are given.

The optical system theory estimates the image quality based on the wide use of the single-point characteristics. These include, among others, spatial resolution (SR).

In this work we have studied the spatial resolution of a system of vision through the atmosphere.

Quantitative and qualitative dependences of the spatial resolution on the detector sensitivity, wavelength, optical thickness, scattering phase function, the presence of atmospheric cloud layers, and the structure of the object has been determined.

Let us examine a vision system formed by the ground, atmosphere, and optical receiver. A solar radiation flux is incident on the top of the atmosphere in the direction specified by the zenith angle θ_0 . Viewing is performed in the nadir from the altitude $L = 90$ km above the ground which is assumed to be Lambertian surface. The object is specified by the albedo distribution.

The notion of the spatial resolution of the object elements was introduced in Ref. 1 based on the Rayleigh criterion as follows. A pair of arbitrary points M_1 and M_2 resolvable by the optical system in the absence of the medium is chosen. It means that there exists at least one point M between M_1 and M_2 for which the following inequality holds:

$$(\tilde{E}_{1,2} - \tilde{E}_M) / (\tilde{E}_{1,2} + \tilde{E}_M) \geq \delta,$$

where $\tilde{E}_{1,2}$ and \tilde{E}_M are the illuminances of the points conjugate to the points M_1, M_2 , and M in the image plane.

It is assumed that in addition to the points M_1 and M_2 the observed object also has m elements located in a random way with respect to M_1 and M_2 . Then in terms of Ref. 1 with solar illumination of the ground, the criterion for resolvability of two points viewed through the atmosphere has the form

$$\gamma_{1,2} = \frac{h_u(a_{1,2}^\lambda E_{1,2}^0 - a_M^\lambda E_M^0) + \sum_{i=1}^m a_i^\lambda E_i^0 (h(r_{1,2;i}) - h(r_{M;i}))}{h_u(a_{1,2}^\lambda E_{1,2}^0 + a_M^\lambda E_M^0) + 2I_p + \sum_{i=1}^m a_i^\lambda E_i^0 (h(r_{1,2;i}) + h(r_{M;i}))} \geq \delta. \quad (1)$$

Here $r_{k;i}$ is the distance from the k th point (subscript $k = 0, 1$, and 2 defines the points M, M_1 and M_2) to the surrounding elements of the object; a_k^λ and a_i^λ are the spectral albedos of the points M, M_1 , and M_2 and

background components; h_u and $h(r_{k,i})$ are the unscattered and scattered components of the point spread function $\tilde{h}(r)$; I_h is the intensity of the solar haze; and E_k^0 and E_i^0 are the illuminances of the corresponding points. Evidently, we must consider only those object elements for which $a_j^\lambda \neq 0 (j = i, k)$.

Let us assume that

$$a_{1,2}^\lambda = A_1^\lambda, \quad a_i^\lambda = A_2^\lambda, \quad E_{1,2}^0 = E_0.$$

Then inequality (1) can be written down as

$$\gamma_{1,2} = \frac{\frac{A_1}{A_2} h_u + \sum_{i=1}^n (h(r_{1,2;i}) - h(r_{M;i}))}{\frac{A_1}{A_2} h_u + \frac{2I_h}{A_2 E_0} + \sum_{i=1}^n (h(r_{1,2;i}) + h(r_{M;i}))} \geq \delta. \quad (2)$$

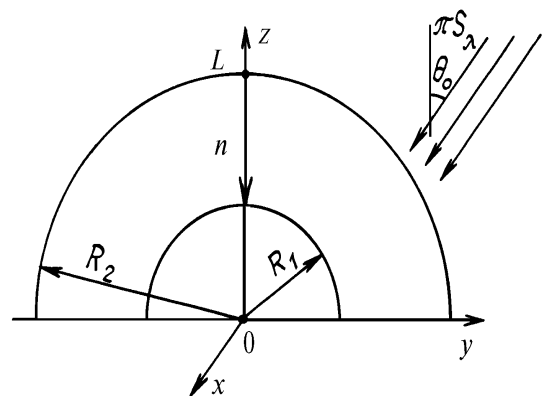


FIG. 1. Geometric scheme of the experiments. R_1 is the Earth's radius, R_2 is the outer radius of the atmosphere.

The spatial resolution of the vision system under study was estimated against criterion (2) by Monte-Carlo simulation of the quantities E_0, \tilde{h} and I_h entering into Eq. (2). The local-estimate algorithm of the adjoint trajectory simulation^{2,4} was employed. The geometry of the simulation is shown in Fig. 1. In numerical experiments a mean cyclic model of the continental aerosol⁵ was employed for the optical model of the atmosphere. The molecular component was taken into account on the basis of McClatchey's data⁶ on the

scattering and extinction coefficients for the mid-latitudes in winter. Two situations were simulated:

- a) cloudless atmosphere,
- b) atmosphere in the presence of a continuous cloud layer of optical depth τ at a height of l km above the ground.

The first situation was studied at the three wavelengths $\lambda = 0.55, 0.86, \text{ and } 1.53 \mu\text{m}$. In the second case, the wavelength was assumed to be $0.55 \mu\text{m}$. The optical properties of the cloud layer were for Deirmenjjan's C1 cloud.⁷ The quantities τ and l took the following values: $\tau = 1, 3, 6, \text{ and } 12$ and $l = 0.25, 1 \text{ and } 2 \text{ km}$. In addition, numerical experiments were performed under conditions of radiation fog layer⁷ of optical depth $\tau = 3$ adjacent to the ground.

Since the analysis of the spatial resolution against criterion (2) cannot be virtually made for objects of arbitrary shape, the numerical estimates of the left side of Eq. (2) were obtained for two specific examples:

- 1) observed object is a set of elements uniformly distributed over the area $S = \pi R_\epsilon^2$ with the albedo A_2 . Here R_ϵ is the radius of the adjacency effect⁴ at $\epsilon = 50\%$;
- 2) sources deteriorating the contrast between M_1 and M_2 are concentrated around M in the form of blocks resembling rings with the average radii \bar{r}_j , and each block contains m_j sources with nonzero albedo A_j . In the particular case $A_j = A_2$ for any j .

The points M_1 and M_2 with albedo A_1 were chosen in the following way. The coordinates of M_1 were $(0, 0, R_1)$, as shown in Fig. 1, while the position of M_2 was determined from the ratio

$$h(M_2)/h(0) = 0.95 .$$

To describe the object of the first type, we considered it expedient to use such a characteristic as the number of sources located in a circle whose diameter d equals the separation between M_1 and M_2 . Evidently, N is related to the coefficient β , introduced in Ref. 1 and taken to mean the average degree of loading of the unit area of the object by the elements of nonzero brightness, by the following equality:

$$\beta = 4N/\pi d^2 .$$

Table I lists the values of d for the examined conditions.

TABLE I. Distance d at $\lambda = 0.55 \mu\text{m}$ for Deirmenjjan's C1 cloud.

τ	1			3			6		
$l, \text{ m}$	250	1000	2000	250	1000	2000	250	1000	2000
$r_{95}, \text{ m}$	1.55	0.95	0.71	2.58	3.65	1.40	2.76	6.27	3.72

Let us examine, as a whole, the behavior of γ and inequality (2) as a function of optical and geometric parameters of the vision system. It should be noted that the increase in the parameter of the left side of Eq. (2)

can always be treated as a potential improvement of the spatial resolution of the vision system. For example, two points of the object become resolvable for a worse detector sensitivity.

On the one hand, the feasibility of spatial resolution against criterion (2) is associated with the factors determining the point spread function, radius of the adjacency effect R , and the ratio $I_h/A_2 E_0$. Among those factors are the optical thickness of the atmosphere, the relative contribution of the aerosol and molecular extinctions, elongation of the scattering phase function, etc. On the other hand, fulfilment of inequality (2) depends on the characteristics of the object. In this case, it depends on the average degree of loading of the unit area of the object β or on the number of rings surrounding the observation points and their loading by the sources deteriorating the contrast, on the relation between the emissivities of the points M_1 and M_2 and their surrounding as well as on the emissivity of the surrounding. It follows from Table II that in the cloudless atmosphere two arbitrary points of the observed objects separated at the distance not smaller than d are resolvable by an optical system whose sensitivity is not worse than $\delta \approx 0.1$ practically regardless of the viewing conditions.

It is obvious, however, that even in the cloudless atmosphere inequality (2) may be violated primarily because the properties of the object vary.

Table II also shows that γ is mainly affected by the ratio A_1/A_2 . For example, for a 1.5–2–fold decrease in γ the average degree of loading β or the ring number N_1 must increase by two or three orders of magnitude, whereas this very effect is attained by a 5–fold decrease in A_1/A_2 . Notably, our calculations show that the spatial resolution of the vision system in the case of annular structure of the object is practically invariant with respect to the albedos of the rings (at least it is true for the examined situations).

Let us dwell on some qualitative dependences. Increase of λ in the wavelength range of interest for mean values of N and N_1 results in higher γ , which is basically associated with the decrease of the optical depth of the vertical atmospheric column. At larger N and N_1 , the monotonic spectral behavior of γ is violated and a minimum is found to occur at $\lambda = 0.86$. In our opinion, the increased number of background reflectors intensifies the effect of scattering properties of the atmosphere, in particular, in its surface layer, on the spatial resolution of the vision system. The characteristics of the vision system (for example, the point spread function and the radius of the adjacency effect) are well known to be strongly dependent on the relative contribution of aerosol and molecular extinction. Though the total optical depth of the atmosphere decreases with increase of λ in the examined wavelength range, the relative contribution of the molecular and aerosol extinctions varies nonmonotonically. Thus, the ratio τ_m/τ_a (τ_m and τ_a are the optical thicknesses of molecular and aerosol extinctions) takes the values of 0.4, 0.14, and 0.67 at $\lambda = 0.55, 0.86, \text{ and } 1.53 \mu\text{m}$, respectively. Apparently, it is this circumstance which causes the above-mentioned behavior of γ .

TABLE II. The values of γ for the cloudless atmosphere.

Object with uniform loading									
$A_1/A_2 = 1$									
$\lambda, \mu\text{m}$	$\tilde{N} = 1$			$\tilde{N} = 100$			$\tilde{N} = 100000$		
	$\theta_0 = 0^\circ$	$\theta_0 = 30^\circ$	$\theta_0 = 60^\circ$	$\theta_0 = 0^\circ$	$\theta_0 = 30^\circ$	$\theta_0 = 60^\circ$	$\theta_0 = 0^\circ$	$\theta_0 = 30^\circ$	$\theta_0 = 60^\circ$
0.55	8.84-01	8.80-01	8.14-01	7.20-01	7.18-01	6.73-01	4.27-03	4.26-03	4.27-03
0.86	9.66-01	9.64-01	9.62-01	5.04-01	5.04-01	5.03-01	1.49-03	1.49-03	1.49-03
1.53	9.84-01	9.89-01	9.90-01	8.35-01	8.39-01	8.40-01	6.00-03	6.00-03	6.00-03
$A_1/A_2 = 0.2$									
$\lambda, \mu\text{m}$	$\tilde{N} = 1$			$\tilde{N} = 100$					
	$\theta_0 = 0^\circ$	$\theta_0 = 30^\circ$	$\theta_0 = 60^\circ$	$\theta_0 = 0^\circ$	$\theta_0 = 30^\circ$	$\theta_0 = 60^\circ$			
0.55	4.34-01	4.26-01	3.03-01	2.79-01	2.75-01	2.19-01			
0.86	7.67-01	7.55-01	7.43-01	1.66-01	1.65-01	1.65-01			
1.53	8.66-01	9.09-01	9.19-01	4.86-01	4.99-01	5.02-01			
Object with annular structure									
$A_1/A_2 = 1$									
$\lambda, \mu\text{m}$	$\tilde{N}_1 = 10$			$\tilde{N}_1 = 100$					
	$\theta_0 = 0^\circ$	$\theta_0 = 30^\circ$	$\theta_0 = 60^\circ$	$\theta_0 = 0^\circ$	$\theta_0 = 30^\circ$	$\theta_0 = 60^\circ$			
0.55	8.62-01	8.60-01	7.96-01	7.03-01	7.33-01	7.32-01			
0.86	8.84-01	8.83-01	8.81-01	4.84-01	4.84-01	4.83-01			
1.53	9.59-01	9.64-01	9.66-01	7.76-01	7.79-01	7.80-01			
$A_1/A_2 = 0.2$									
$\lambda, \mu\text{m}$	$\tilde{N}_1 = 10$			$\tilde{N}_1 = 100$					
	$\theta_0 = 0^\circ$	$\theta_0 = 30^\circ$	$\theta_0 = 60^\circ$	$\theta_0 = 0^\circ$	$\theta_0 = 30^\circ$	$\theta_0 = 60^\circ$			
0.55	4.10-01	4.02-01	2.93-01	2.66-01	2.63-01	2.11-01			
0.86	5.62-01	5.55-01	5.49-01	1.55-01	1.54-01	1.54-01			
1.53	7.79-01	8.13-01	8.21-01	3.97-01	4.05-01	4.07-01			

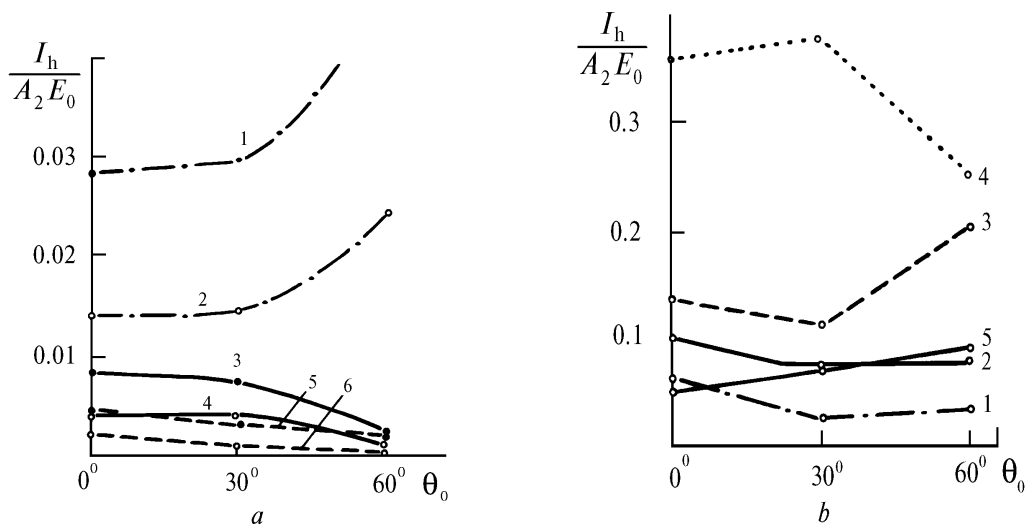


FIG. 2. Dependence of the ratio I_h/A_2E_0 on the solar zenith angle: open circles are for $A_1/A_2 = 1$ and dots are for $A_1/A_2 = 0.2$. a) cloudless atmosphere: dot-dash lines are for $\lambda = 0.55 \mu\text{m}$, solid lines are for $\lambda = 0.86 \mu\text{m}$, and dashed lines are for $\lambda = 1.53 \mu\text{m}$; b) curves 1-4 are for C1 cloud, $l = 250 \text{ m}$; curve 5 is for the surface fog, curve 1 is for $\tau = 1$, curves 2 and 5 are for $\tau = 3$, curve 3 is for $\tau = 6$, and curve 4 is for $\tau = 12$. $\lambda = 0.55 \mu\text{m}$.

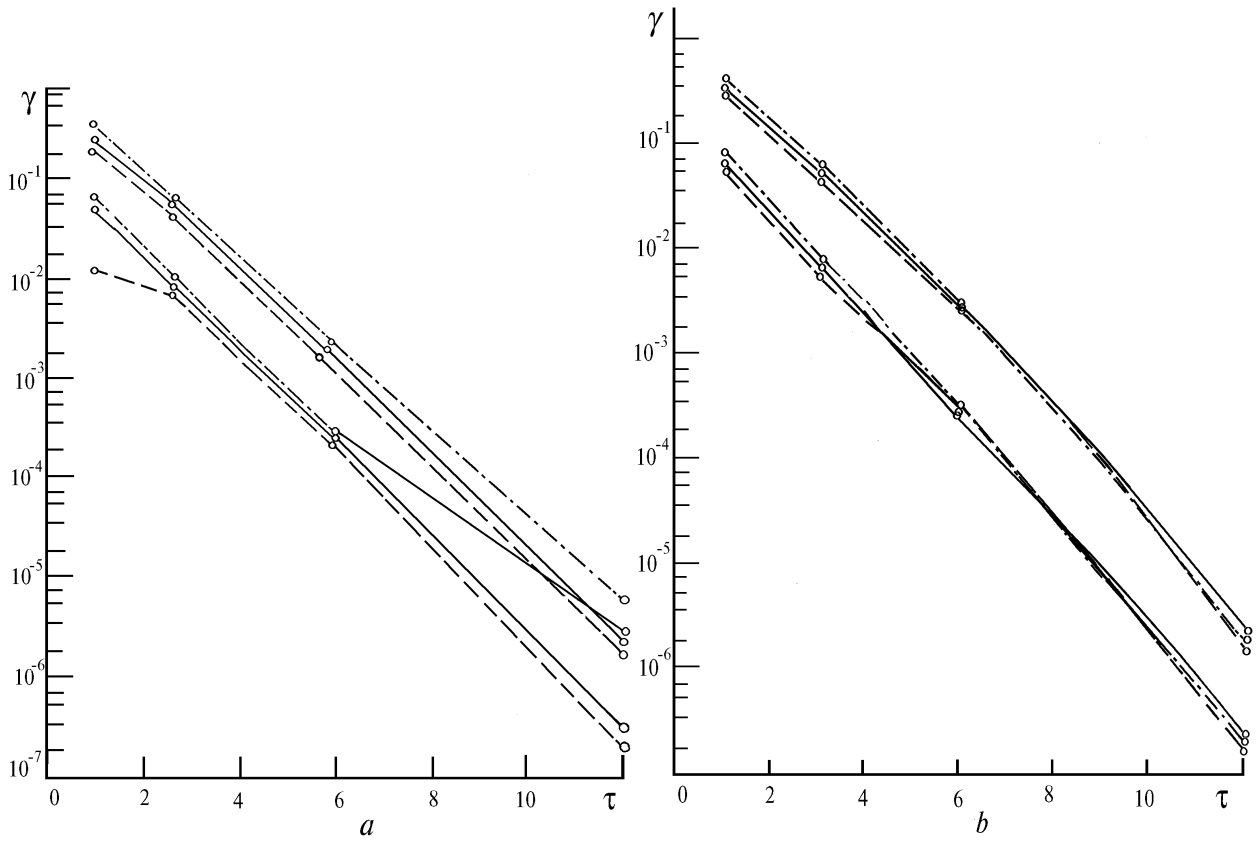


FIG. 3 Dependence of γ on the optical depth of the cloud layer: open circles are for $A_1/A_2 = 1$, dots are for $A_1/A_2 = 0.2$, dot-dash lines are for $l = 250$ m, solid lines are for $l = 1$ km, dashed lines are for $l = 2$ km, a) object with uniform degree of loading, $\tilde{N} = 1$; b) object with annular structure, $N_1 = 10$.

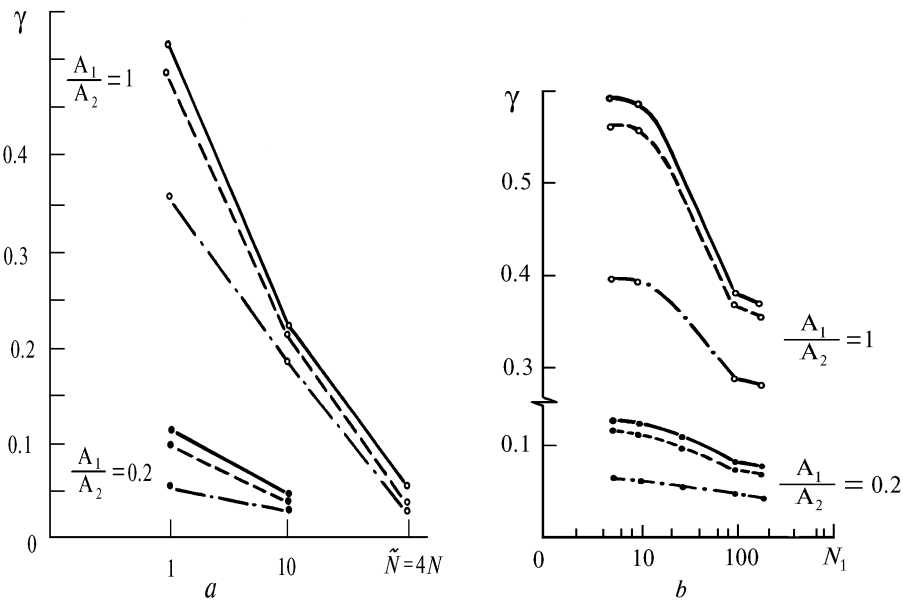


FIG. 4. Dependence of γ on the number of background reflectors: C1 cloud is at the height l ; $\tau = 1$. Dash-dot lines are for $\theta_0 = 0^\circ$, dashed lines are for $\theta_0 = 30^\circ$, and solid lines are for $\theta_0 = 60^\circ$, a) object with a uniform degree of loading at $l = 250$ m; b) object with annular structure at $l = 1$ km.

It follows from Eq. (2) that the effect of the solar zenith angle on the spatial resolution of the vision system is determined by the ratio I_h/A_2E_0 . The latter (see Fig. 2a) is a monotonic function of the solar zenith angle θ_0 for the cloudless atmosphere. It is either increasing or decreasing function depending on the wavelength, which correspondingly affects the behavior of $\gamma_{1,2}$ (Table II). It should be noted that the correlation of the qualitative dependences of $\gamma(\theta_0)$ and $I_h/A_2E_0(\theta_0)$ at $\lambda = 0.86$ differs from the analogous correlation at the other wavelengths. In our opinion, this fact may also result from a larger contribution of the aerosol extinction at this very wavelength.

In addition, the data in Table II indicate that the dependence of the spatial resolution on the solar zenith angle virtually vanishes as the number of background elements increases. The presence of dense layers in the atmosphere associated primarily with an increased total optical thickness causes not only a substantial decrease of γ , but also changes certain qualitative trends. The validity of criterion (2) in this case is to a far greater degree dependent on the characteristic features of the radiation extinction and scattering in the atmosphere. Our previous study⁸ shows that the point spread function, the radius of the adjacency effect, and the intensity of the solar haze I_h strongly depend on such characteristics of an enhanced turbidity layer as the optical thickness, scattering phase function, and the location of this layer on the viewing path. Our calculations show that the degree of spatial resolution in the presence of a cloud layer is primarily determined by its optical thickness. To a lesser degree the spatial resolution is determined by the scattering phase function and the height of the lower boundary of the layer (within the ranges of variation of the corresponding parameters). It can be seen from Figs. 3a and b that the increase in the optical thickness leading first of all to a several-fold increase in I_h is accompanied by a sharp decrease of $\gamma_{1,2}$.

Vertical displacement of the continuous cloud layer from the ground somehow deteriorates the spatial resolution of the vision system.

At $\tau \approx 12$ the spatial resolution in accordance with criterion (2) is feasible, provided the detector sensitivity is not worse than $\delta \approx 10^{-6}$ – 10^{-7} depending on the albedo.

Figures 4a and b depict γ at three solar zenith angles for two values of A_1/A_2 . Note the most pronounced dependence of the left side of inequality (2) on the solar zenith angle, which is anticorrelated, as in the case of the cloudless atmosphere, with the dependence of I_h/A_2E_0 on θ_0 (Fig. 2b). A comparison of the plots shown in Figs. 4 and 5 indicates that the effect of the solar zenith angle on the degree of spatial resolution of the vision system decreases as the optical thickness of the enhanced turbidity layer increases.

On the basis of Figs. 3, 4, and 5 we can make certain conclusions about the effect of the shape of the observed object on the degree of spatial resolution of vision systems. Specific features inherent in the formations of the point spread function and the domain of the adjacency effect are responsible for the largest differences between the values of γ for the objects under consideration when the enhanced turbidity layer is located near the ground (Fig. 5). In addition, the difference between the values of γ increases with the number of the background points of objects.

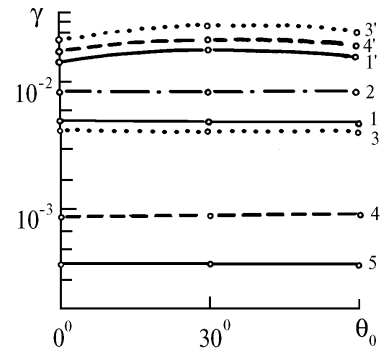


FIG. 5. Dependence of γ on the solar zenith angle for objects of different structures. $A_1/A_2 = 1$. Curves 1–5 are for the surface fog; curves 1', 3', and 4' are for C1 cloud at the height $l = 250$ m; curves 1, 1', and 2 are for the object with a uniform degree of loading; curves 3, 3', 4, 4', and 5 are for the object with annular structure; curves 1 and 1' are for $N_1 = 10$; curve 2 is for $N_1 = 100$; curves 3 and 3' are for $\tilde{N} = 1$; curves 4 and 4' are for $\tilde{N} = 10$; and, curve 5 is for $\tilde{N} = 100$. $\tau_{ob} = \tau_t = 3$.

Summarizing, it can be concluded that

1. Spatial resolution of systems of vision through the atmosphere is feasible even in the presence of optically dense layers provided that the detector has an adequate sensitivity.
2. In the presence of an atmospheric cloud layer, the solar zenith angle $\theta_0 \approx 30^\circ$ appears to be most optimum (against criterion (2)) for observations.
3. The dependence of the degree of spatial resolution of the vision system on the structure of the observed object in the presence of an enhanced turbidity layer in the atmosphere is most pronounced when the layer is adjacent to the ground.

REFERENCES

1. V.V. Belov, Opt. Atm. **1**, No. 9, 17–24 (1988).
2. G.I. Marchuk, et al., *The Monte Carlo Method in Atmospheric Optics* (Springer–Verlag, Berlin, 1980).
3. V.V. Belov and I.Yu. Makushkina, in: *Theory and Applications of Statistical Simulation*, Computing Center of the Siberian Branch of the Academy of Sciences of the USSR, Novosibirsk (1988), pp. 153–164.
4. V.V. Belov and I.Yu. Makushkina, in: *Image Transfer in the Earth's Atmosphere*, Tomsk Affiliate of the Siberian Branch of the Academy of Sciences of the USSR, Tomsk (1988), pp. 3–10.
5. G.M. Krekov and R.F. Rakhimov, *Optical Models of Atmospheric Aerosols*, Tomsk Affiliate of the Siberian Branch of the Academy of Sciences of the USSR, Tomsk (1986), 294 pp.
6. R.A. McClatchey, R.W. Fenn, J.E. Selby, et al., *Optical Properties of the Atmosphere (Revised)*, Report AFCRL–77–0272, AFCRL, Bedford, Mass. (1971), 98 pp.
7. D. Deirmendjian, *Electromagnetic Scattering on Spherical Polydispersions* (Elsevier, Amsterdam; American Elsevier, New York, 1969).
8. V.V. Belov and I.Yu. Makushkina, Opt. Atm. **1**, No. 2, 18–24 (1988).